Research Square

Preprints are preliminary reports that have not undergone peer review.
They should not be considered conclusive, used to inform clinical practice,
or referenced by the media as validated information.

Partially coherent beams shaping in uniaxial crystal orthogonal to optical axis

H. Nabil
Hassan First University of Settat, Ecole Nationale des Sciences Appliquées, LISA
M. Bayraktar
University of Luxembourg
S. Chatzinotas
University of Luxembourg
A. Balhamri
Hassan First University of Settat, Ecole Nationale des Sciences Appliquées, LISA
A. Belafhal
belafhal@gmail.com
Chouib Doukali University

Research Article

Keywords: Laguerre Bessel Gaussian Schell model, Crystal optics, Refractive index, Cross-spectral density

Posted Date: June 16th, 2026

DOI: https://doi.org/10.21203/rs.3.rs-9866390/v1

License: This work is licensed under a Creative Commons Attribution 4.0 International License.
Read Full License

Additional Declarations: No competing interests reported.

Version of Record: A version of this preprint was published at Optical and Quantum Electronics on September 11th, 2026. See the published version at https://doi.org/10.1007/s11082-026-09143-1.

Partially coherent beams shaping in uniaxial crystal orthogonal to optical axis

H. Nabil[1,2], M. Bayraktar[3], S. Chatzinotas[3], A. Balhamri[1], A. Belafhal[2*]

[1]Hassan First University of Settat, Ecole Nationale des Sciences Appliquées, LISA, 26100 Berrechid, Morocco

[2]Laboratory LPNAMME, Laser Physics Group, Departements of Physics,

Faculty of Sciences, Chouib Doukali University, P. B 20, 24000 El Jadida, Morocco

[3]Interdisciplinary Centre for Security, Reliability, and Trust (Snt), University of Luxembourg,

Luxembourg City L-1855, Luxembourg

Corresponding author. E-mail: belafhal@gmail.com

H. Nabil: nabilmasterpmc@gmail.com/

M. Bayraktar: mert.bayraktar@uni.lu/S. Chatzinotas: symeon.chatzinotas@uni.lu/

A. Balhamri: adil.balhamri@gmail.com/A. Belafhal: belafhal@gmail.com

Abstract

In this work, we introduced and investigated the behavior propagation of a partially coherent Laguerre-Bessel-Gaussian Schell model (PCLBGSM) beam inside uniaxial crystal orthogonal to an optical axis. The analytical formulas for the cross spectral density function, spectral density, and degree of coherence are derived. The impact of source beam and uniaxial crystal parameters on the shape of spectral density and degree of coherence are analyzed numerically. The results reveal that the propagating beam exhibits a dark hollow shape with adjustability of the source beam and uniaxial crystal parameters. From our main expressions, we found the particular cases, and we note that our results closely align with those found in the previous literature. The outcomes suggest the potential applications in optical manipulation.

Keywords: *Laguerre Bessel Gaussian Schell model; Crystal optics; Refractive index; Cross-spectral density.*

1. Introduction

The role of crystal materials in compensator, polarizer, amplitude, and phase modulation design devices makes them intriguing. To design these devices and distinguish the structure of uniaxial crystals, it is crucial to do research on how optical fields propagate in uniaxial anisotropic crystals (Ciattoni et al. 2002; Ciattoni et al. 2001; Fleck and Feit 1983; Izdebskaya et al. 2009; M. Born and E. Wolf; Stamnes and Sherman 1976). The theoretical approach describing the electromagnetic beams propagating in a uniaxial crystal based on solving Maxwell's equation in anisotropic materials, which investigates the beams oriented perpendicularly to the optical axis has been developed by Ciattoni et al. (Ciattoni and Palma

2003). From then on, various coherent beams spreading behaviors in uniaxial crystals have been reported, like as Laguerre-Gaussian, Hermite-Gaussian, Bessel-Gaussian beams, hollow Gaussian, flattened Gaussian, cylindrically polarized vector, Airyprime beams, hyperbolic sinusoidal Gaussian beams, double half inverse Gaussian hollow beams, and Laguerre higher order cosh Gaussian (Bayraktar 2021; Bayraktar 2020; Benzehoua et al. 2024; Cincotti et al. 2002a; Cincotti et al. 2002b; Deng et al. 2008; Li et al. 2013; Lü and Luo 2004; Yaalou et al. 2025).

However, partially coherent beams can effectively reduce the speckle effect of a beam compared with fully coherent ones. They have been employed for various applications, specifically in optical trapping, laser scanning, and free-space optical communication. Thus, the latter beam's behavior inside a uniaxial crystal have been discussed, such as multi Gaussian Schell model (Lu et al. 2016), rectangular multi Gaussian Schell model (Mao and Mei 2017), beams carrying an edge dislocation (Li et al. 2020), and partially polarized partially coherent Gaussian Schell model (Liu and Zhou 2009).

A new beam the Laguerre Gaussian and Bessel Gaussian Schell model, exhibits some remarkable propagation features in far field ring shape (Mei and Korotkova 2013). They are appropriate for particle trapping applications and can be generated experimentally (Avramov-Zamurovic et al. 2016; Gangireddy et al. 2013; Wang et al. 2013). After that, their spreading through various media has drawn a lot of interest. Cang et al. investigated the spreading behavior of the average intensity and the beam width of the Laguerre-Gaussian and Bessel-Gaussian Schell beams through a paraxial ABCD optical system in Kolmogorov turbulence (Cang et al. 2013). Wang et al. reported the evolution features of the Bessel Gaussian Schell model beam in non-Kolmogorov turbulence by using the propagation factor, the degree of coherence, and the effective radius of curvatures (Wang et al. 2015). Wu et al. studied and analyzed the impact of the source beam and oceanic turbulence on the evolution of average intensity and directionality of a Gaussian Schell model, Bessel-Gaussian Schell model beams and Laguerre-Gaussian Schell model (Wu et al. 2016b). In another work, Wu et al. presented an average intensity and spreading model for Gaussian Schell model, Bessel-Gaussian Schell model beams, and Laguerre-Gaussian Schell model in the turbulence of the biological tissue (Wu et al. 2016a). Zhou et al. generated a Bessel-Gaussian shell model beam and analyzed its scintillation index in a weak atmosphere (Zhou et al. 2020). Another approach to the spreading feathers inside uniaxial crystals of a Laguerre-Gaussian correlated Schell-model beam has been developed by Zhu et al. (Zhu et al. 2015). In this context, recently our research group has been contributing (Chib et al. 2022a; Chib et al. 2022b; Ebrahim et al. 2025; Nabil et al. 2024; Nabil

et al. 2022a; Nabil et al. 2022b). Motivate by the previous work, we introduce the Laguerre-Bessel-Gaussian Schell model (PCLBGSM) beam, which can be considered as a general case of a Bessel-Gaussian Schell model beams and Laguerre-Gaussian Schell model. This beam possesses a ring-shaped far field; these properties may make it more suitable for particle manipulation.

This work studies the propagation behaviors of a PCLBGSM beam in a uniaxial crystal orthogonal to the optical axis. This work is structured as follows: firstly, we derived the theoretical framework in section 2. Then the propagation behaviors of the beam's spectral density (SD) and degree of coherence (DOC), together with interpretation, are examined in Section 3 using numerical simulations. Finally, the last section provides a summary of the outcomes.

2. Theory

We consider a beam propagating in the direction of the z axis, and the optical axis of the uniaxial crystal consists with the x axis. Dielectric tensor of uniaxial crystal can be taken as

$$\varepsilon = \begin{pmatrix} n_e^2 & 0 & 0 \\ 0 & n_o^2 & 0 \\ 0 & 0 & n_o^2 \end{pmatrix}, \tag{1}$$

where $n_i \ \left(i = o, e\right)$ denote the refractive indices of the ordinary and extraordinary.

Using the paraxial approximation, the spreading of a laser beam inside a uniaxial crystal obeys the following equations (Ciattoni and Palma 2003)

$$E_x\left(\boldsymbol{\rho}, z\right) = \frac{k_0 n_o}{2i\pi z}\exp\left(ik_0 n_e z\right)\iint E_x\left(\boldsymbol{r}, 0\right)\exp\left\{\frac{ik_0}{2zn_e}\left(n_o^2\left(\rho_x - x\right)^2 + n_e^2\left(\rho_y - y\right)^2\right)\right\}dxdy, \tag{2}$$

$$E_y\left(\boldsymbol{\rho}, z\right) = \frac{k_0 n_o}{2i\pi z}\exp\left(ik_0 n_e z\right)\iint E_y\left(\boldsymbol{r}, 0\right)\exp\left\{\frac{ik_0 n_o}{2z}\left(\left(\rho_x - x\right)^2 + \left(\rho_y - y\right)^2\right)\right\}dx\,dy, \tag{3}$$

where $\boldsymbol{r} = \left(x, y\right)$ and $\boldsymbol{\rho} = \left(\rho_x, \rho_y\right)$ presents the position vectors in the source and receiving plane, respectively. $k_0 = 2\pi/\lambda$ is the wavenumber related with wavelength. The input and the output planes' electric fields are denoted by $E_i\left(\boldsymbol{r}, 0\right)$ and $E_i\left(\boldsymbol{\rho}, 0\right)\left(i = x, y\right)$.

At the source plane, the cross-spectral density function (CSD) of a PCLBGSM beam can be formulated as follow (Mandel and Wolf 1995)

$$W\left(\boldsymbol{r}_1, \boldsymbol{r}_2, 0\right) = \exp\left\{-\frac{\boldsymbol{r}_1^2 + \boldsymbol{r}_2^2}{4\sigma_0^2}\right\}\eta^{(0)}\left(\boldsymbol{r}_1 - \boldsymbol{r}_2\right), \tag{4}$$

where σ_0 represents the beam width. With $\eta^{(0)}$ takes the following form

$$\eta^{(0)}\left(\boldsymbol{r}_1-\boldsymbol{r}_2\right)=\exp\left(-\frac{\left(\boldsymbol{r}_1-\boldsymbol{r}_2\right)^2}{2\delta_0^2}\right)L_n\left(\frac{\left(\boldsymbol{r}_1-\boldsymbol{r}_2\right)^2}{2\delta_0^2}\right)J_0\left(\frac{\beta\left|\boldsymbol{r}_1-\boldsymbol{r}_2\right|}{\delta_0}\right), \tag{5}$$

where δ_0 refer to source coherence width and β is the real constant. L_n is the Laguerre polynomial with order *n*, and $J_0(\cdot)$ is the zero order Bessel function. Eq. (5) can be reduced to the particular cases: if $\beta=0$, we can find Laguerre-Gaussian shell model beam (Mei and Korotkova 2013), if *n*=0, Bessel-Gaussian shell model beam (Mei and Korotkova 2013), and if $n=\beta=0$, the Gaussian shell model beam.

Referring to the paraxial propagation, the laser beam propagating inside a uniaxial crystal can be evaluated by the correlation function of the field between two arbitrary points $\boldsymbol{\rho}_1=\left(\rho_{1x},\rho_{1y}\right)$ and $\boldsymbol{\rho}_2=\left(\rho_{2x},\rho_{2y}\right)$ are expressed as

$$\begin{aligned}W\left(\boldsymbol{\rho}_1,\boldsymbol{\rho}_2,z\right)=\frac{k_0^2n_o^2}{4\pi^2z^2}\int_{-\infty}^{+\infty}\int_{-\infty}^{+\infty}W\left(\boldsymbol{r}_1,\boldsymbol{r}_2,0\right)\exp\left\{\frac{ik_0}{2zn_e}\left(n_o^2\left(x_1-\rho_{x_1}\right)^2+n_e^2\left(y_1-\rho_{y_1}\right)^2\right)\right\}\\ \times\exp\left\{-\frac{ik_0}{2zn_e}\left(n_o^2\left(x_2-\rho_{x_2}\right)^2+n_e^2\left(y_2-\rho_{y_2}\right)^2\right)\right\}d^2\boldsymbol{r}_1d^2\boldsymbol{r}_2.\end{aligned} \tag{6}$$

To evaluate the latter equation, the integration variables are changed by making

$$\boldsymbol{\rho}_s=\boldsymbol{\rho}_1+\boldsymbol{\rho}_2/2,\quad \boldsymbol{\rho}_d=\boldsymbol{\rho}_1-\boldsymbol{\rho}_2, \tag{7a}$$

$$\boldsymbol{r}_s=\boldsymbol{r}_1+\boldsymbol{r}_2/2,\quad \boldsymbol{r}_d=\boldsymbol{r}_1-\boldsymbol{r}_2. \tag{7b}$$

Then Eq. (6) can be rewritten as

$$\begin{aligned}W\left(\boldsymbol{\rho}_s,\boldsymbol{\rho}_d,z\right)=\frac{k_0^2n_o^2}{4\pi^2z^2}\int_{-\infty}^{+\infty}\int_{-\infty}^{+\infty}\int_{-\infty}^{+\infty}\int_{-\infty}^{+\infty}W\left(\boldsymbol{r}_s,\boldsymbol{r}_d,0\right)\exp\left\{\frac{in_o^2k_0}{2zn_e}\left(2x_sx_d+2\rho_{sx}\rho_{dx}-2x_s\rho_{dx}-2x_d\rho_{sx}\right)\right\}\\ \times\exp\left\{\frac{in_ek_0}{2z}\left(2y_sy_d+2\rho_{sy}\rho_{dy}-2y_s\rho_{dy}-2y_d\rho_{sy}\right)\right\}d^2\boldsymbol{r}_sd^2\boldsymbol{r}_d,\end{aligned} \tag{7c}$$

with

$$W\left(\boldsymbol{r}_s,\boldsymbol{r}_d,0\right)=\exp\left[-\frac{\boldsymbol{r}_s^2}{2\sigma_0^2}-\left(\frac{1}{8\sigma_0^2}+\frac{1}{2\delta_0^2}\right)\boldsymbol{r}_d^2\right]L_n\left(\frac{\boldsymbol{r}_d^2}{2\delta_0^2}\right)J_0\left(\frac{\beta\left|\boldsymbol{r}_d\right|}{\delta_0}\right). \tag{7d}$$

Then, after some tedious computations, one obtains the important analytical expression function of a PCLBGSM beam within a uniaxial crystal as

$$
\begin{aligned}
W\left(\boldsymbol{\rho}_s,\boldsymbol{\rho}_d,z\right)=&\frac{k_0^2 n_o^2\sigma_0^2}{2z^2}\exp\left\{-\frac{k_0^2\left(\delta_0^2+4\sigma_0^2\right)\left(n_o^4 M_y\rho_{dx}^2+n_e^4 M_x\rho_{dy}^2\right)}{16n_e^2 z^2\delta_0^2 M_x M_y}\right\}\\
&\times\exp\left\{\frac{ik_0\left(\delta_0^2+4\sigma_0^2\right)\left(n_o^2 M_y\rho_{sx}\rho_{dx}+n_e^2 M_x\rho_{sy}\rho_{dy}\right)}{8n_e z\sigma_0^2\delta_0^2 M_x M_y}\right\}\exp\left\{-\frac{k_0^2\left(n_o^4 M_y\rho_{sx}^2+n_e^4 M_x\rho_{sy}^2\right)}{4n_e^2 z^2 M_x M_y}\right\}\\
&\times\sum_{p=0}^{n}\sum_{m=0}^{p}\binom{n}{p}\binom{p}{m}\frac{1}{2^{3p}\,p!\,\delta_0^{2p}}\sum_{l=0}^{\infty}\sum_{q=0}^{l}\binom{l}{q}\frac{\beta^{2l}}{2^{4l}\left(l!\right)^2\delta_0^{2l}}\frac{1}{M_x^{p-m+l-q+\frac{1}{2}}M_y^{m+q+\frac{1}{2}}}\\
&\times H_{2(p-m+l-q)}\left(\frac{n_o^2 k_0}{2zn_e\sqrt{M_x}}\left(\rho_{sx}+\frac{in_o^2 k_0\sigma_0^2}{zn_e}\rho_{dx}\right)\right)\\
&\times H_{2(m+q)}\left(\frac{n_e k_0}{2z\sqrt{M_y}}\left(\rho_{sy}+\frac{in_e k_0\sigma_0^2}{z}\rho_{dy}\right)\right),
\end{aligned}
\tag{8}
$$

where

$$
M_x=\frac{1}{8\sigma_0^2}+\frac{1}{2\delta_0^2}+\frac{n_o^4 k_0^2\sigma_0^2}{2z^2 n_e^2},
\tag{9a}
$$

and

$$
M_y=\frac{1}{8\sigma_0^2}+\frac{1}{2\delta_0^2}+\frac{n_e^2 k_0^2\sigma_0^2}{2z^2}.
\tag{9b}
$$

In the above derivation of Eq. (8), we have used the following integral and expansion expressions (Belafhal et al. 2021; I. S. Gradshteyn, I. M. Ryzhik 2007)

$$
L_n\left(x\right)=\sum_{p=0}^{n}\binom{n}{p}\frac{\left(-1\right)^p}{p!}x^p,
\tag{10a}
$$

$$
J_0\left(x\right)=\sum_{l=0}^{\infty}\frac{\left(-1\right)^l x^{2l}}{2^{2l}\left(l!\right)^2},
\tag{10b}
$$

$$
\left(x+y\right)^n=\sum_{m=0}^{n}\binom{n}{m}x^{n-m}y^m,
\tag{10c}
$$

$$
\int\exp\left(-\frac{1}{2}px^2+qx\right)dx=\sqrt{\frac{2\pi}{p}}\exp\left(\frac{q^2}{2p}\right),
\tag{10d}
$$

and

$$
\int x^n e^{-px^2+2qx}dx=e^{q^2/p}\sqrt{\frac{\pi}{p}}\left(\frac{1}{2i\sqrt{p}}\right)^n H_n\left(\frac{iq}{\sqrt{p}}\right).
\tag{10e}
$$

Our study focuses on the distributions of the SD and DOC of a PCLBGSM beam inside a uniaxial crystal. By setting $\boldsymbol{\rho}_1 = \boldsymbol{\rho}_1 = \boldsymbol{\rho}$ in Eq. (8), the SD is yield as

$$\begin{aligned} S(\boldsymbol{\rho},z) = {} & \frac{k_0^2 n_o^2 \sigma_0^2}{2z^2} \exp\left(-\frac{k_0^2 n_o^4 M_y}{4 n_e^2 z^2 M_x M_y} \rho_x^2 - \frac{k_0^2 n_e^4 M_x \rho_y^2}{4 n_e^2 z^2 M_x M_y} \rho_y^2 \right) \\ & \times \sum_{p=0}^{n} \sum_{m=0}^{p} \binom{n}{p} \binom{p}{m} \frac{1}{2^{3p}\, p! \delta_0^{2p}} \sum_{l=0}^{\infty} \sum_{q=0}^{l} \binom{l}{q} \frac{\beta^{2l}}{2^{4l} (l!)^2 \delta_0^{2l}} \frac{1}{M_x^{p-m+l-q+\frac{1}{2}} M_y^{m+q+\frac{1}{2}}} \\ & \times H_{2(p-m+l-q)}\left(\frac{n_o^2 k_0}{2 z n_e \sqrt{M_x}} \rho_{sx} \right) H_{2(m+q)}\left(\frac{n_e k_0}{2z\sqrt{M_y}} \rho_{sy} \right). \end{aligned} \tag{11}$$

The spectral DOC can be given as follows

$$\eta^{(0)} = \frac{W(\boldsymbol{\rho}_1, \boldsymbol{\rho}_2, z)}{\sqrt{S(\boldsymbol{\rho}_1, z)} \sqrt{S(\boldsymbol{\rho}_2, z)}}. \tag{12}$$

The analytical expression of the Eqs. (8), (11), and (12) are the main result of the current work. This work is a general study; it allows us to produce certain new studies as special cases expressed as follows

- **Propagation of a Laguerre Gaussian Schell model beam**

If we make $l = \beta = 0$, in Eq. (8), one obtains

$$\begin{aligned} W(\boldsymbol{\rho}_s, \boldsymbol{\rho}_d, z) = {} & \frac{k_0^2 n_o^2 \sigma_0^2}{2z^2} \exp\left\{ -\frac{k_0^2 \left(n_o^4 M_y \rho_{sx}^2 + n_e^4 M_x \rho_{sy}^2 \right)}{4 n_e^2 z^2 M_x M_y} \right\} \\ & \times \exp\left\{ -\frac{k_0^2 \left(\delta_0^2 + 4\sigma_0^2 \right) \left(n_o^4 M_y \rho_{dx}^2 + n_e^4 M_x \rho_{dy}^2 \right)}{16 n_e^2 z^2 \delta_0^2 M_x M_y} \right\} \\ & \times \exp\left\{ \frac{i k_0 \left(\delta_0^2 + 4\sigma_0^2 \right) \left(n_o^2 M_y \rho_{sx} \rho_{dx} + n_e^2 M_x \rho_{sy} \rho_{dy} \right)}{8 n_e z \sigma_0^2 \delta_0^2 M_x M_y} \right\} \\ & \times \sum_{p=0}^{n} \sum_{m=0}^{p} \binom{n}{p} \binom{p}{m} \frac{1}{2^{3p}\, p! \delta_0^{2p}} \frac{1}{M_x^{p-m+\frac{1}{2}} M_y^{m+\frac{1}{2}}} \\ & \times H_{2p-2m}\left(\frac{n_o^2 k_0}{2 z n_e \sqrt{M_x}} \left(\rho_{sx} + \frac{i n_o^2 k_0 \sigma_0^2}{z n_e} \rho_{dx} \right) \right) H_{2m}\left(\frac{n_e k_0}{2z\sqrt{M_y}} \left(\rho_{sy} + \frac{i n_e k_0 \sigma_0^2}{z} \rho_{dy} \right) \right). \end{aligned} \tag{13}$$

the finding Eq. (13) is seen as a special case of our current investigation and is accord with Eq. (11) of the Ref. (Zhu et al. 2015).

- **Propagation of a Bessel Gaussian Schell model beam**

By setting $n=0$, in Eq. (8), one obtains

$$
\begin{aligned}
W\left(\boldsymbol{\rho}_s,\boldsymbol{\rho}_d,z\right)=&\frac{k_0^2 n_o^2\sigma_0^2}{2z^2}\exp\left\{-\frac{k_0^2\left(n_o^4 M_y\rho_{sx}^2+n_e^4 M_x\rho_{sy}^2\right)}{4n_e^2 z^2 M_x M_y}\right\}\\
&\times\exp\left\{-\frac{k_0^2\left(\delta_0^2+4\sigma_0^2\right)\left(n_o^4 M_y\rho_{dx}^2+n_e^4 M_x\rho_{dy}^2\right)}{16n_e^2 z^2\delta_0^2 M_x M_y}\right\}\\
&\times\exp\left\{\frac{ik_0\left(\delta_0^2+4\sigma_0^2\right)\left(n_o^2 M_y\rho_{sx}\rho_{dx}+n_e^2 M_x\rho_{sy}\rho_{dy}\right)}{8n_e z\sigma_0^2\delta_0^2 M_x M_y}\right\}\\
&\times\sum_{l=0}^{\infty}\sum_{q=0}^{l}\binom{l}{q}\frac{\beta^{2l}}{2^{4l}\left(l!\right)^2\delta_0^{2l}}\frac{1}{M_x^{l-q+\frac{1}{2}}M_y^{q+\frac{1}{2}}}\\
&\times H_{2(l-q)}\left(\frac{n_o^2 k_0}{2zn_e\sqrt{M_x}}\left(\rho_{sx}+\frac{in_o^2 k_0\sigma_0^2}{zn_e}\rho_{dx}\right)\right)H_{2q}\left(\frac{n_e k_0}{2z\sqrt{M_y}}\left(\rho_{sy}+\frac{in_e k_0\sigma_0^2}{z}\rho_{dy}\right)\right),
\end{aligned}
\tag{14}
$$

Eq. (14) is a new expression; it allows to study behavior of the propagation of Bessel Gaussian Schell model beam in uniaxial crystal.

- **Propagation of Gaussian Schell model beam**

By making $n=l=\beta=0$, one finds

$$
\begin{aligned}
W\left(\boldsymbol{\rho}_s,\boldsymbol{\rho}_d,z\right)=&\frac{k_0^2 n_o^2\sigma_0^2}{2z^2}\exp\left\{-\frac{k_0^2\left(\delta_0^2+4\sigma_0^2\right)\left(n_o^4 M_y\rho_{dx}^2+n_e^4 M_x\rho_{dy}^2\right)}{16n_e^2 z^2\delta_0^2 M_x M_y}\right\}\\
&\times\exp\left\{\frac{ik_0\left(\delta_0^2+4\sigma_0^2\right)\left(n_o^2 M_y\rho_{sx}\rho_{dx}+n_e^2 M_x\rho_{sy}\rho_{dy}\right)}{8n_e z\sigma_0^2\delta_0^2 M_x M_y}\right\}\exp\left\{-\frac{k_0^2\left(n_o^4 M_y\rho_{sx}^2+n_e^4 M_x\rho_{sy}^2\right)}{4n_e^2 z^2 M_x M_y}\right\}.
\end{aligned}
\tag{15}
$$

3. Numerical example and analysis

According to the analytical formula derived above, we present in this section some numerically simulation about the propagation behavior of a PCLBGSM beam inside the uniaxial crystals. The calculation parameters are chosen to be $\lambda=623.8nm$, $\sigma_0=20\,\mu m$, $\delta_0=5\mu m$, $\beta=5$, $n=2$, $z_R=\pi\sigma_0^2/\lambda$ and $n_o=2.616$. The spectral density distribution of the PCLBGSM for different values of the source coherence width at the propagation distances ($z=0$, $z=z_R$, $z=2z_R$, and $z=10z_R$) is shown in Fig. 1. On can show that the coherence width influences the spectral density shape. If the source coherent width is small, the spectral density

shape quickly changes from Gaussian to elliptical dark hollow. As the source coherent width increases, the received spectral density will change their shape more slowly. We can observe the central dark region increases while propagation distances raise.

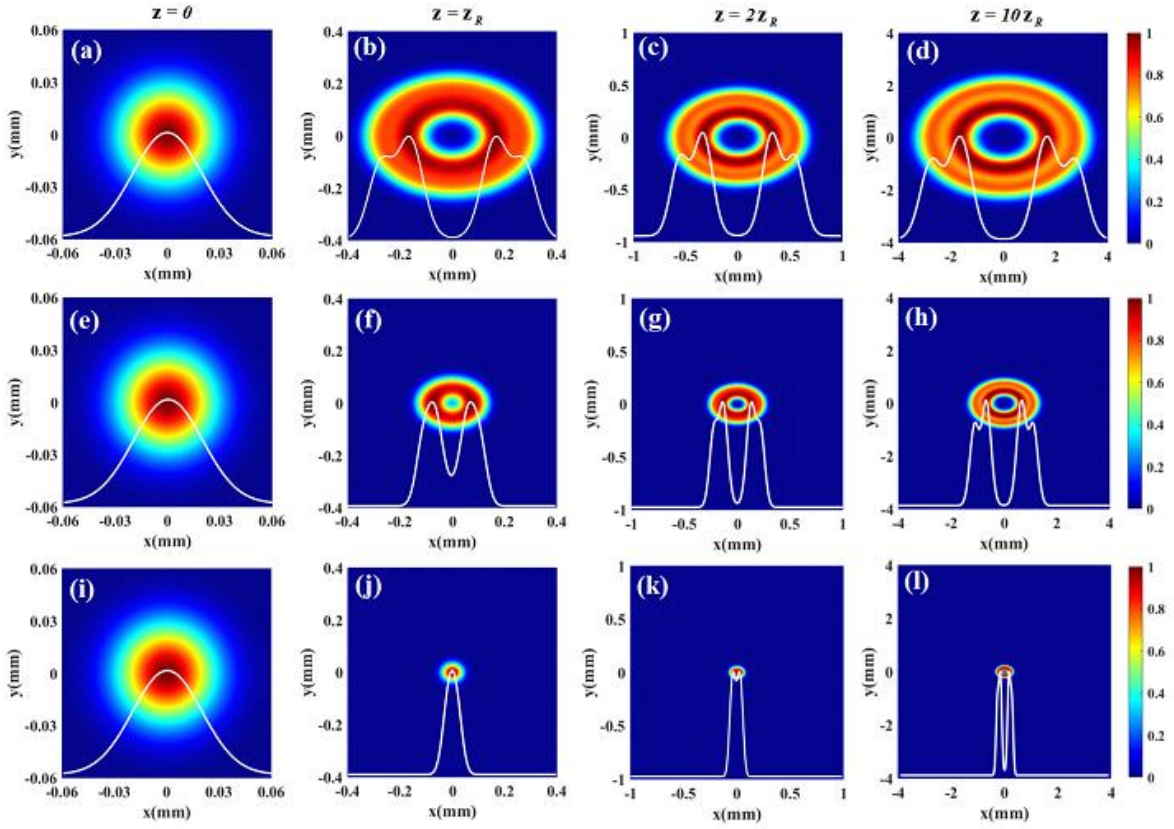


Figure 1: Spectral density of PCLBGSM with different coherent widths:

$\delta_0 = 2\mu m$ (a-d), $\delta_0 = 5\mu m$ (e-h), and $\delta_0 = 20\mu m$ (i-l).

The SD distribution of a PCLBGSM beam inside uniaxial crystal by varying distances of propagation for various values of parameter β, with source coherent width $\delta_0 = 5\mu m$, is given in Fig. 2. As we increase the parameter β, the beam shape evolves to elliptical dark hollow. We also note that, as the propagation distance grows, the beam has a large central dark hollow.

To carry out the influence of uniaxial crystal, we show in Fig .3, the spectral density evolution of a PCLBGSM inside uniaxial crystal by changing ratio of the refractive index n_e/n_o. As shown in this figure, the evolution of PCLBGSM inside isotropic crystal are differs greatly from that of an anisotropic crystal, it is related to the ratio of the refractive index i.e. changing the material.

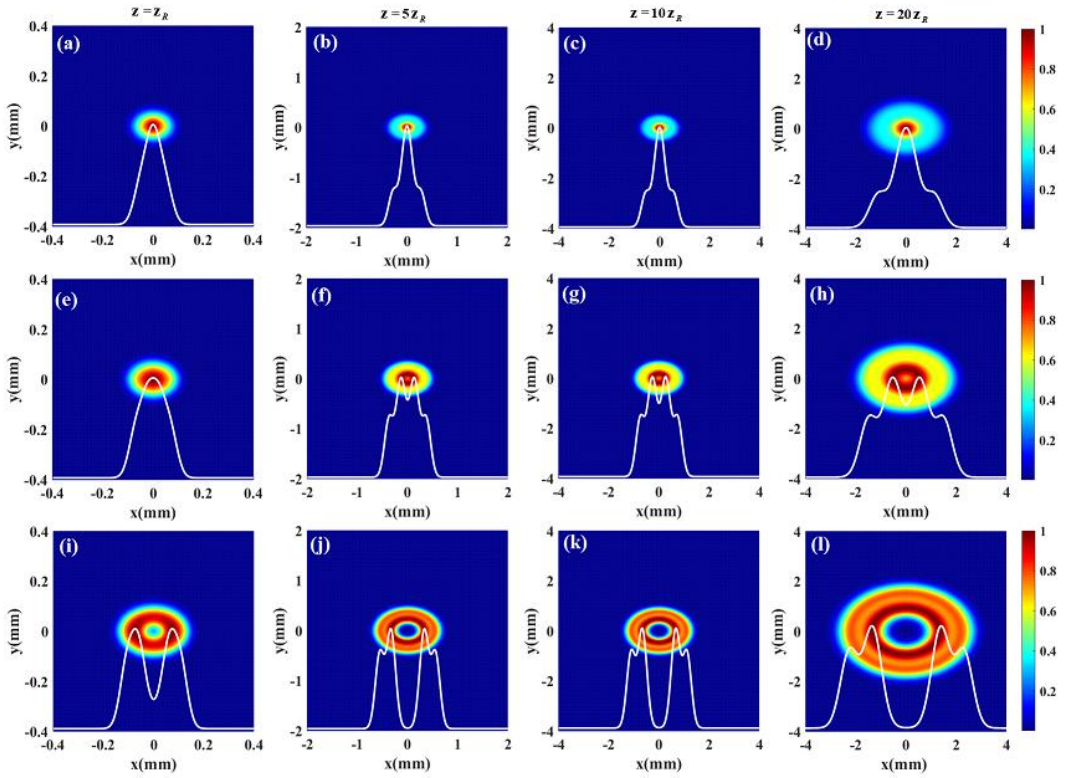


Figure 2: SD of PCLBGSM through uniaxial crystal with different parameters (a-d) $\beta = 2$, (e-h) $\beta = 3$ and (i-l) $\beta = 5$.

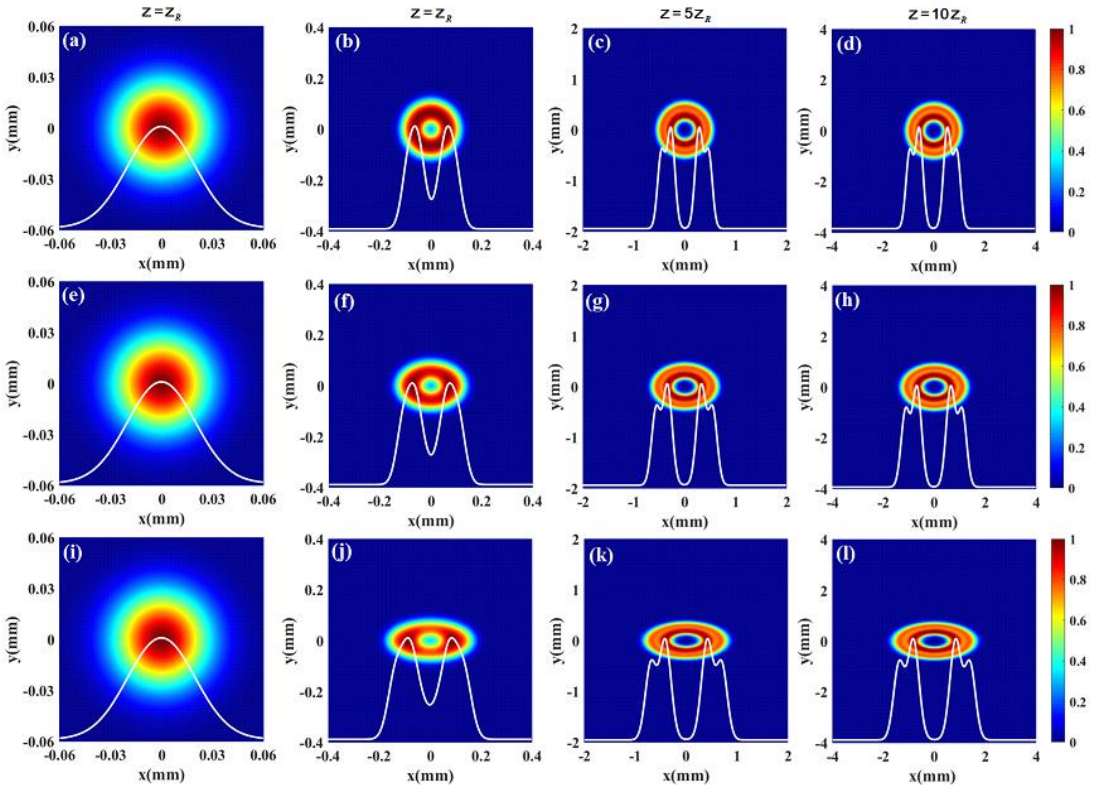


Figure 3: SD of PCLBGSM beam in a uniaxial crystal with different parameters of n_e/n_o:

(a-d) $n_e/n_o = 1$, (e-h) $n_e/n_o = 1.2$ and (i-l) $n_e/n_o = 1.5$.

With the increase of the parameter n_e/n_o the spectral density profile becomes more elliptical i.e. more astigmatic due to anisotropic diffraction. Thus, a source coherent width, the parameter β, and the ratio of refractive index plays a crucial role for determining and modulating the spectral density shape.

To learn more about the behavior of a PCLBGSM beam through uniaxial crystal, we analyze the behavior of the DOC. The influence of the parameter β and the order *n* on the behavior of the DOC of a PCLBGSM beam inside uniaxial crystal are depicted in Figs. 4 and (5). One can see that, the degree of coherence has the different lobes with larger beam order *n* and the parameter β. In addition, at large enough propagation distance, regardless of beam order *n* and parameter β, the lobes will vanish.

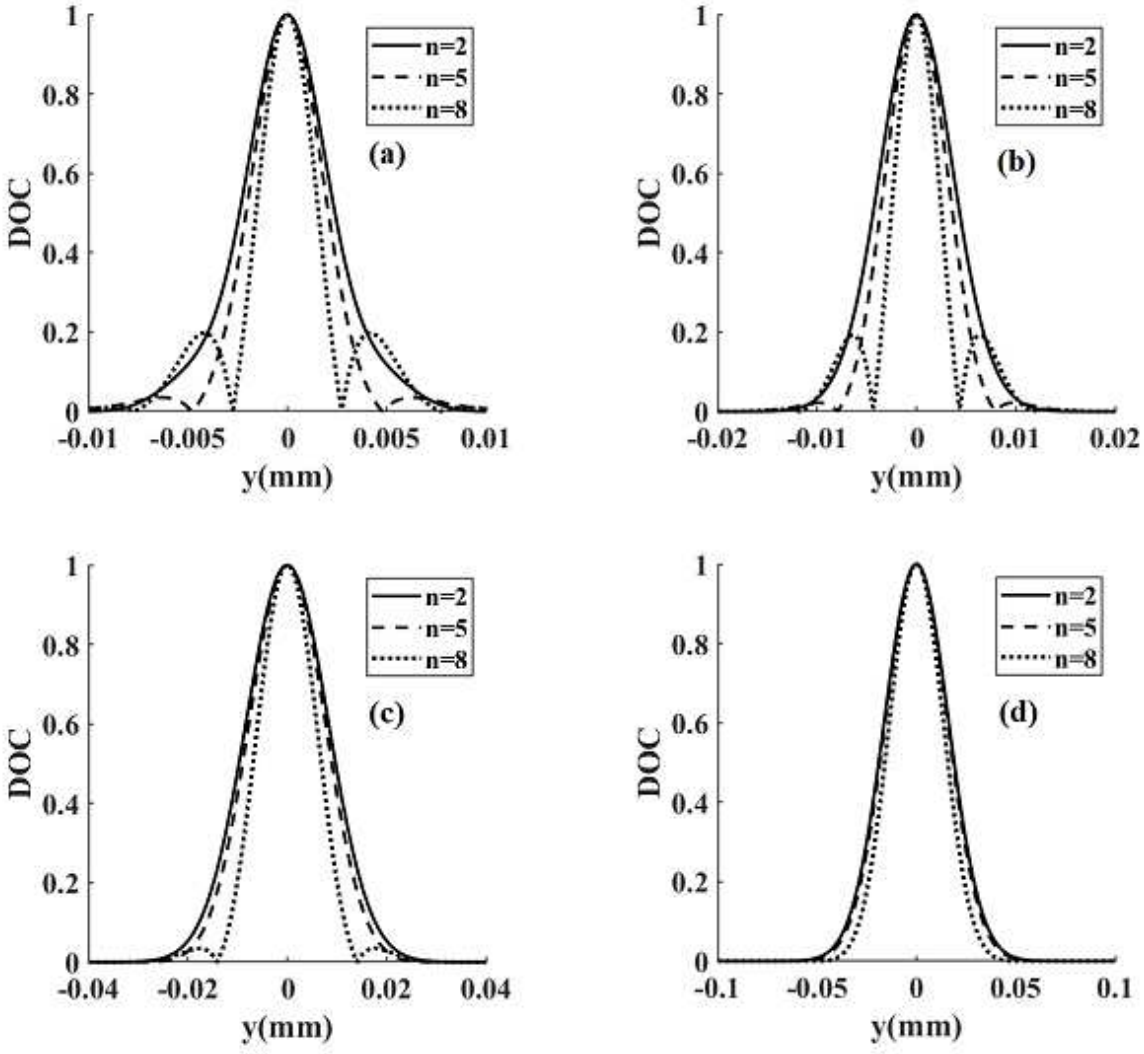


Figure 4: DOC of a PCLBGSM beam with different parameter beam orders *n* at various propagation distances: $z = z_R$ **(a)**, $z = 2z_R$ **(b)**, $z = 5z_R$ **(c)**, and $z = 10z_R$ **(d)**.

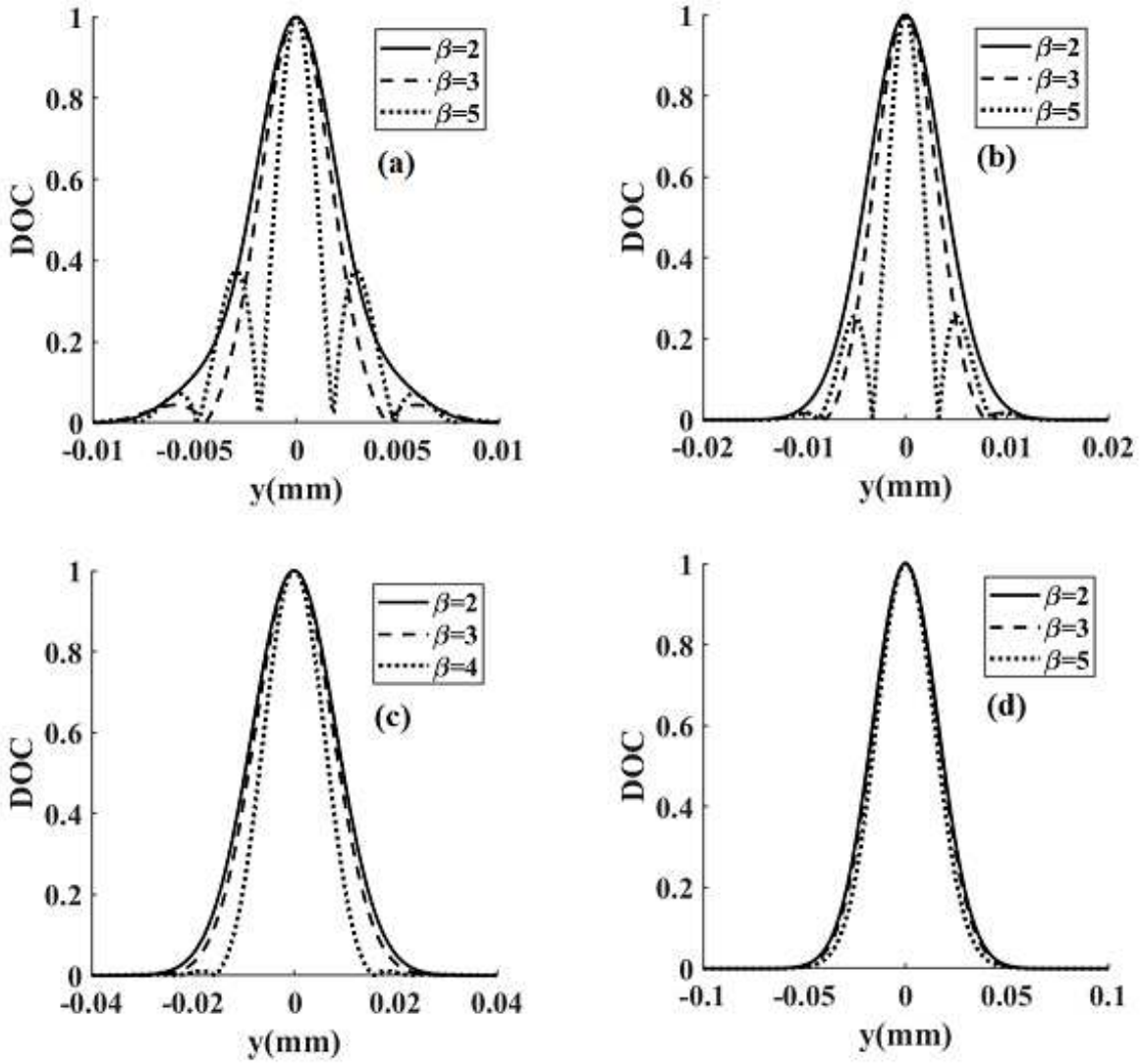


Figure 5: DOC of a PCLBGSM beam with different parameters β at various distances:

$z = z_R$ **(a)**, $z = 2z_R$ **(b)**, $z = 5z_R$ **(c)**, and $z = 10z_R$ **(d).**

Fig. 6 represents the evolution of the DOC of a PCLBGSM inside uniaxial crystal versus propagation distances by varying the ratio refractive index n_e/n_o (see Fig. 6a) and for different pairs of points the coherence located symmetrically (see Fig. 6b). In Fig. 6a, the degree of coherence is analyzed by using the pairs of points (10,0) and (-10,0). One can see from Fig. 6a that the DOC will first increase with increases in the ratios of refractive index at a given plane z, but in the far field, the DOC is nearly the same for different ratios of refractive index. In Fig. 6b, at the source, we may observe that the DOC is different for various point correlation, as the distance of propagation increase the difference of the DOC of different points will eventually disappear, especially in the far field.

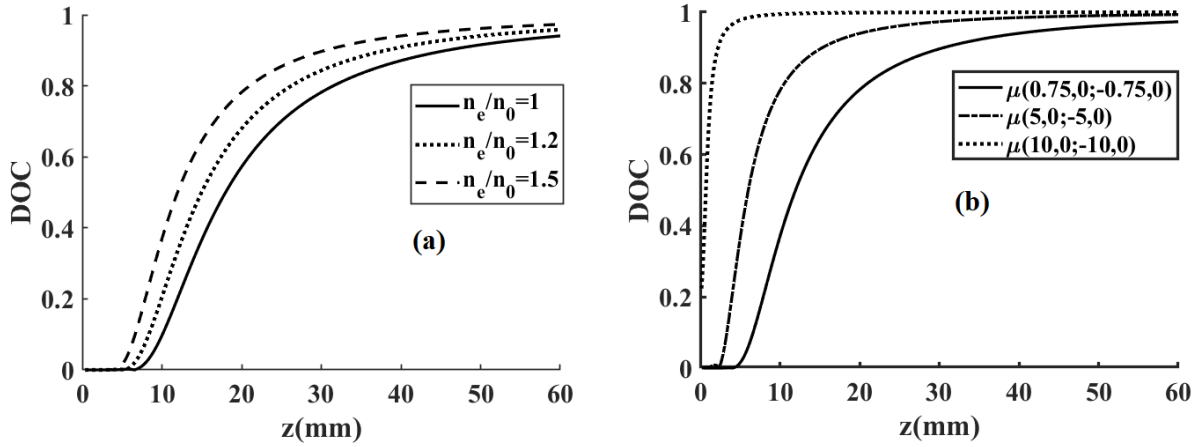


Figure 6: DOC versus z of a PCLBGSM beam at different values of:

(a) n_e/n_o with n=5, $\beta = 2$ and **(b)** points the correlation with $n_e/n_o = 1.5$, n=5, $\beta = 2$.

In Fig. 7, we use Eq. (13) to illustrate the SD of a Laguerre Gaussian Schell model beam through uniaxial crystal. We can observe from the plot of this figure that the results obtained are in good accord with those of the Ref. (Zhu et al. 2015) (see Fig. 1). Furthermore, our study is more generalized because the outcomes of Ref. (Zhu et al. 2015) are considered as a specific case of the current study.

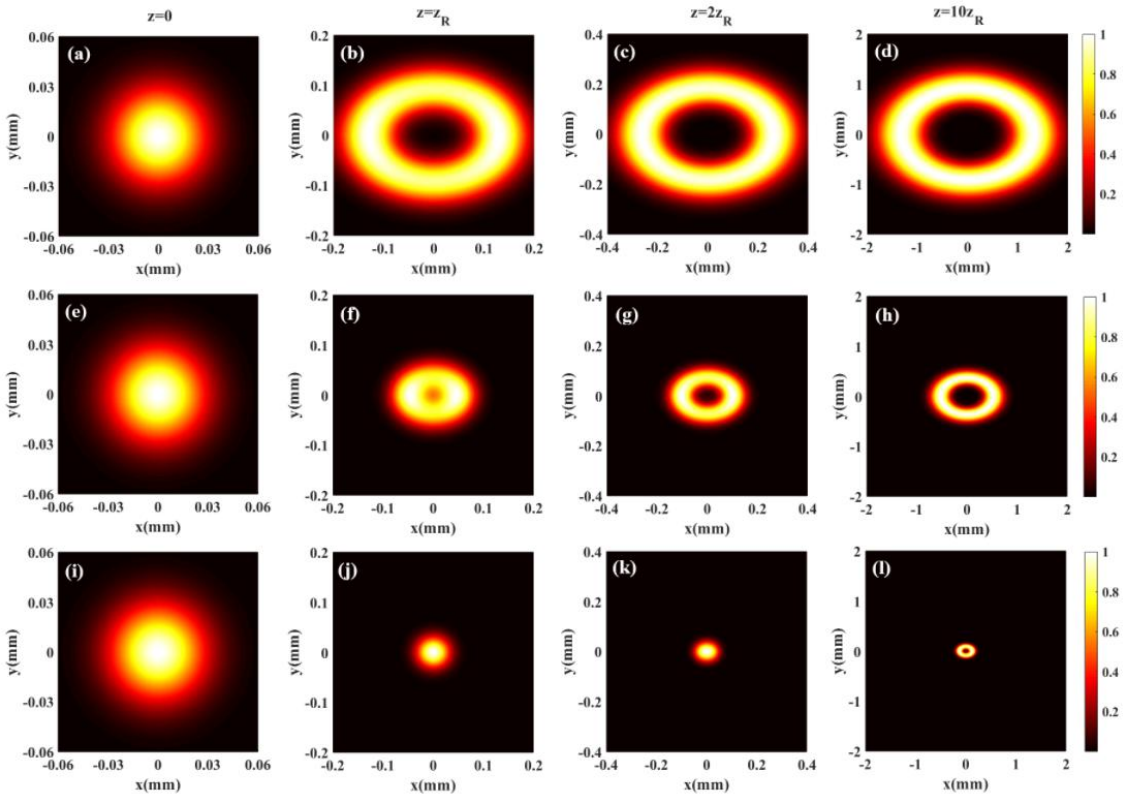


Figure 7: SD of PCLGSM beam in a uniaxial crystal with different values of the coherent width:

$\delta_0 = 2\mu m$ **(a-d)**, $\delta_0 = 5\mu m$ **(e-h)**, and $\delta_0 = 20\mu m$ **(i-l).**

4. Conclusion

As a result, we have obtained the analytical formulas for the CSD function, SD and DOC of a PCLBGSM beam inside uniaxial crystal. By using numerical calculation, we study the influence of the initial beam parameter and the uniaxial crystal on the SD and the DOC of a PCLBGSM. We found that the spectral density changes rapidly their shape to elliptical dark hollow with lower source coherence width, higher parameter β. In addition, we found that the corresponding beam becomes more elliptical as the ratios of index refractive increase. At short propagation distance, the degree of coherence is influenced more by mode order n, parameter β and the ratios of index refractive than far field. From our main analytical and numerical results, we derived the particular cases such as Laguerre-Gaussian shell model, Bessel-Gaussian shell model and Gaussian shell model. It will be noted that our finding agrees well with those published in literature. Our study may be useful in optical manipulation.

Declarations

Ethical Approval

This article does not contain any studies involving animals or human participants performed by any of the authors. We declare this manuscript is original, and is not currently considered for publication elsewhere. We further confirm that the order of authors listed in the manuscript has been approved by all of us.

Competing interests

The authors have no financial or proprietary interests in any material discussed in this article.

Authors' contributions

All authors contributed to the study conception and design. All authors performed simulations, data collection and analysis and commented the present version of the manuscript. All authors read and approved the final manuscript.

Funding: No funding is received from any organization for this work.

Availability of data and materials

No datasets are used in the present study.

Consent for publication

The authors confirm that there is informed consent to the publication of the data contained in the article.

Consent to participate

Informed consent was obtained from all authors.

References

Avramov-Zamurovic, S., Nelson, C., Guth, S., Korotkova, O., Malek-Madani, R.: Experimental study of electromagnetic Bessel-Gaussian Schell Model beams propagating in a turbulent channel. Optics Communications. 359, 207–215 (2016).

Bayraktar, M.: Propagation of Airyprime beam in uniaxial crystal orthogonal to propagation axis. Optik. 228, 166183 (1–8) (2020).

Bayraktar, M.: Propagation of hyperbolic sinusoidal Gaussian beams in uniaxial crystals orthogonal to the optical axis. Optik. 233, 166613 (1–11) (2021).

Belafhal, A., Chib, S., Khannous, F., Usman, T.: Evaluation of integral transforms using special functions with applications to biological tissues. Comp. Appl. Math. 40, 156 (1–23) (2021).

Benzehoua, H., Saad, F., Belafhal, A.: The characteristics of Laguerre higher-order cosh-Gaussian beam propagating in uniaxial crystal orthogonal to the optical axis. Optical and Quantum Electronics. 56, (1–16) (2024).

Cang, J., Xiu, P., Liu, X.: Propagation of Laguerre–Gaussian and Bessel–Gaussian Schell-model beams through paraxial optical systems in turbulent atmosphere. Optics & Laser Technology. 54, 35–41 (2013).

Chib, S., Dalil-Essakali, L., Belafhal, A.: Effects of turbulent atmosphere on the spectral density of Bessel-modulated Gaussian Schell-model beams. Optical and Quantum Electronics. 54, 468 (1–12) (2022)(a).

Chib, S., Dalil-Essakali, L., Belafhal, A.: Comparative analysis of some Schell-model beams propagating through turbulent atmosphere. Optical and Quantum Electronics. 54, 175 (1–17) (2022)(b).

Ciattoni, A., Cincotti, G., Palma, C.: Ordinary and extraordinary beams characterization in uniaxially anisotropic crystals. Optics Communications. 195, 55–61 (2001).

Ciattoni, A., Cincotti, G., Palma, C.: Nonparaxial description of reflection and transmission at the interface between an isotropic medium and a uniaxial crystal. Journal of the Optical Society of America A. 19, 1422–1431 (2002).

Ciattoni, A., Palma, C.: Optical propagation in uniaxial crystals orthogonal to the optical axis: paraxial theory and beyond. Journal of the Optical Society of America A. 20, 2163–2171 (2003).

Cincotti, G., Ciattoni, A., Palma, C.: Laguerre–Gauss and Bessel–Gauss beams in uniaxial crystals. Journal of the Optical Society of America A. 19, 1680–1688 (2002)(a).

Cincotti, G., Ciattoni, A., Palma, C.: Hermite-Gauss beams in uniaxially anisotropic crystals. IEEE Photonics Journal. 37, 1517–1524 (2002)(b).

Deng, D., Yu, H., Xu, S., Shao, J., Fan, Z.: Propagation and polarization properties of hollow Gaussian beams in uniaxial crystals. Optics Communications. 281, 202–209 (2008).
Ebrahim, A.A.A., Saad, F., Mohammed, A.A., Belafhal, A.: Analysis of propagation characteristics of a partially coherent modified anomalous vortex beam in uniaxial crystals. Optical and Quantum Electronics. 57, 412 (2025).
Fleck, J.A., Feit, M.D.: Beam propagation in uniaxial anisotropic media. Journal of the Optical Society of America A. 73, 920–926 (1983).
Gangireddy, S., Kumar, A., Prabhakar, S., Singh, R.: Experimental generation of ring-shaped beams with random sources. Optics Letters. 38, 4441–4444 (2013).
I. S. Gradshteyn, I. M. Ryzhik: Table of integrals, series, and products. (2007).
Izdebskaya, Y., Brasselet, E., Shvedov, V., Desyatnikov, A., Królikowski, W., Kivshar, Y.: Dynamics of linear polarization conversion in uniaxial crystals. Optics Express. 17, 18196–18208 (2009).
Li, J., Chen, Y., Cao, Q.: Propagation properties of cylindrically polarized vector beam through uniaxial crystals along the optical axis. Optics & Laser Technology. 45, 364–372 (2013).
Li, L., Jiang, C., Huan, Y., Wang, H., Liu, D., Wang, Y.: Influences of uniaxial crystal on partially coherent beams carrying an edge dislocation. Optik. 202, 163736 (1–12) (2020).
Liu, D., Zhou, Z.: Propagation of partially polarized, partially coherent beams in uniaxial crystals orthogonal to the optical axis. European Physical Journal D. 54, 95–101 (2009).
Lü, B., Luo, S.: Propagation properties of three-dimensional flattened Gaussian beams in uniaxially anisotropic crystals. Optics & Laser Technology. 36, 51–56 (2004).
Lu, X., Shen, Y., Zhu, X., Zhao, C., Cai, Y.: Evolution properties of multi-Gaussian Schell model beams propagating in uniaxial crystal orthogonal to the optical axis. 46, 19–34 (2016).
M. Born and E. Wolf: Principles of Optics. Pergamon, Oxford, UK, 1999.
Mandel, L., Wolf, E.: Optical Coherence and Quantum Optics. Cambridge University Press, Cambridge (1995)
Mao, Y., Mei, Z.: Propagation Properties of the Rectangular Multi-Gaussian Schell-Model Beams in Uniaxial Crystals Orthogonal to the Optical Axis. IEEE Photonics Journal. 9, 1–11 (2017).
Mei, Z., Korotkova, O.: Random sources generating ring-shaped beams. Optics Letters. 38, 91-93 (2013).
Nabil, H., Balhamri, A., Bayraktar, M., Chatzinotas, S., Belafhal, A.: Impact of joint turbulence of jet engine and marine environment on the propagation quality of partially coherent

generalized Laguerre–Gaussian correlated Schell model beams. Optical and Quantum Electronics. 56, 8081–26 (2024).

Nabil, H., Balhamri, A., Belafhal, A.: Propagation of Bessel-Gaussian Shell-model beam through a jet engine exhaust turbulence. Optical and Quantum Electronics. 54, 232–352 (2022)(a).

Nabil, H., Balhamri, A., Belafhal, A.: Propagation of the Laguerre-Gaussian correlated Shell-model beams through a turbulent jet engine exhaust. Optical and Quantum Electronics. 54, 231–249 (2022)(b).

Stamnes, J.J., Sherman, G.C.: Radiation of electromagnetic fields in uniaxially anisotropic media. Journal of the Optical Society of America A, 66, 780–788 (1976).

Wang, F., Liu, X., Yuan, Y., Cai, Y.: Experimental generation of partially coherent beams with different complex degrees of coherence. Optics Letters. 38, 1814–1816 (2013).

Wang, X., Yao, M., Qiu, Z., Yi, X., Liu, Z.: Evolution properties of Bessel-Gaussian Schell-model beams in non-Kolmogorov turbulence. Optics Express. 23, 12508–12523 (2015).

Wu, Y., Zhang, Y., Wang, Q., Hu, Z.: Average intensity and spreading of partially coherent model beams propagating in a turbulent biological tissue. Journal of Quantitative Spectroscopy and Radiative Transfer. 184, 308–315 (2016)(a).

Wu, Y., Zhang, Y., Zhu, Y.: Average intensity and directionality of partially coherent model beams propagating in turbulent ocean. Journal of the Optical Society of America A. 33, 1451–1458 (2016)(b).

Yaalou, M., Lazrek, M., Hricha, Z., Belafhal, A.: Evolution characteristics of double-half inverse gaussian hollow beams in uniaxial crystals. Optical and Quantum Electronics. 57, 1–12 (2025).

Zhou, Z., Zhou, X., Yuan, X., Tian, P.: Research on characteristics of Bessel–Gaussian Schell-model beam in weak turbulence. Optics Communications. 474, 126074 (1–7) (2020).

Zhu, Z., Liu, L., Wang, F., Cai, Y.: Evolution properties of a Laguerre–Gaussian correlated Schell-model beam propagating in uniaxial crystals orthogonal to the optical axis. Journal of the Optical Society of America A. 32, 374–380 (2015).